Dimensioning Flat Circular Radiating Panels for Plane Wave Generation

Amedeo Capozzoli*, Claudio Curcio*, Lars Foged†, Angelo Liseno*, Francesco Saccardi†

*Dipartimento di Ingegneria Elettrica e delle Tecnologie dell'Informazione (DIETI),
Università di Napoli Federico II,
Via Claudio 21, 80125 Napoli, Italy.
a.capozzoli@unina.it

†Microwave Vision Group (MVG) Italy,
via Castelli Romani, 59,
Pomezia (Italy)
lars.foged@mvg-world.com

***Abstract*—This work addresses the dimensioning of circular radiating panels designed to reproduce prescribed multi-frequency fields within a spherical Quiet Zone (QZ). Relying on the Singular Value Decomposition (SVD) analysis of the radiation operator, the proposed method enforces field synthesis constraints over a planar Quiet Plane (QP) parallel to the panel and determines the minimal panel size required to generate the desired field subspace. Numerical results demonstrate the accuracy of the synthesized fields and validate the effectiveness of the proposed dimensioning strategy across the frequency band of interest.**

***Index Terms*—Dimensioning, Radiating Panel, Plane Wave Generators (PWGs), Singular Value Decomposition (SVD), Quiet Zone, Quiet Plane.**

I. Introduction

The design of radiating panels capable of generating prescribed fields in their Near-Field (NF) zones is relevant in a wide range of applications [1]–[6]. In radar testing, radiating panels are used to emulate canonical target echoes [3], [7], while, in electromagnetic compatibility, equivalent sources are introduced to reproduce the NFs of printed circuit boards [4]. More recently, over-the-air testing has renewed the interest in Plane Wave Generators (PWGs) [5], [6], which employ suitably arranged antenna arrays to approximate plane waves in their NF and thus enable far-field (FF) testing at practical distances.

In this paper, we address the dimensioning problem, namely the determination of the size of a radiating surface $\mathcal{S}'$ that reproduces multi-frequency plane waves in a Quiet Zone (QZ). The objective is pursued by enforcing the desired field behavior on a constraint domain $\mathcal{D}$, typically a planar region intersecting the QZ, chosen to guarantee performance throughout the whole QZ. The fields radiated on $\mathcal{D}$ must approximate the desired plane waves with bounded error over the operational band $\mathcal{B}$.

We follow the developments of an approach exploiting the Singular Value Decomposition (SVD) of the operator linking the panel to the radiated fields [1], [2] and which allows to identify the effective radiating subspaces and set the panel dimensions accordingly, particularized to the case of plane waves.

Indeed, we extend the methodology introduced in [8] to the case of a circular radiating panel, relevant for PWG applications, restricting the analysis to a scalar formulation of the problem. The QZ is modeled as a spherical region centered on the panel, while the constraint domain $\mathcal{D}$ is a planar Quiet Plane (QP) parallel to it.

Numerical results provide a first assessment of the approach.

II. The problem

The problem geometry is illustrated in Fig. 1.

The flat circular panel $\mathcal{S}'$ has radius a' while the QZ $\mathcal{V}$ is spherical, with radius a_R and centered at a distance d apart from the radiating panel. The QP is the flat, rectangular region $\mathcal{D} = [-a, a] \times [-b, b]$ located at a distance d' from $\mathcal{S}'$. The problem is determining the minimum radius a' to radiate fields belonging to $\mathcal{T}(f)$, for $f \in \mathcal{B}$.

A. The Panel Operator

We consider a scalar source distribution $J(x', y'; f)$ supported on the radiating surface $\mathcal{S}'$. Its contribution to the field observed on the constraint region $\mathcal{D}$ is described by the operator $\mathcal{A}_f$, which maps, for a fixed frequency f, the panel current J into the radiated field $E(x, y; f)$:

$$\mathcal{A}_f : \; J(x', y'; f) \; \mapsto \; E(x, y; f), \quad (x, y) \in \mathcal{D}. \qquad (1)$$

B. Relevant Spaces

1) The Approximating Space: To characterize the radiating capabilities of the panel, we employ the singular system of $\mathcal{A}_f$:

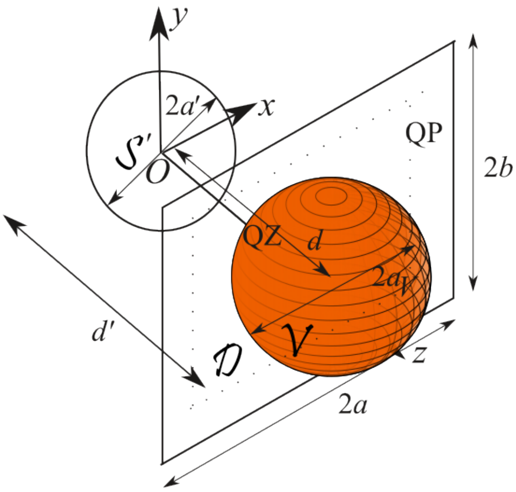

Fig. 1. Geometry of the problem.

$$\{\sigma_p^{\mathcal{A}_f}(f),\ u_p^{\mathcal{A}_f}(x',y';f),\ v_p^{\mathcal{A}_f}(x,y;f)\}_{p=1}^{P(f)}, \tag{2}$$

where $\sigma_p^{\mathcal{A}_f}(f)$ are the singular values, the $u_p^{\mathcal{A}_f}(x',y';f)$ and $v_p^{\mathcal{A}_f}(x,y;f)$ are the right and left singular functions expanding the source and the radiated field on $\mathcal{D}$, respectively. Since the singular spectrum typically exhibits a sharp decay, only the first $P(f)$ terms are relevant for the singular value expansion of $\mathcal{A}_f$. The truncated expansion defines the effective subspace of the fields radiated by the panel [9].

Accordingly, the subspace of fields made available by the panel at frequency f is

$$\mathcal{P}(f) = \{v_p^{\mathcal{A}_f}(x,y;f)\}_{p=1}^{P(f)}. \tag{3}$$

2) The Target Space: The desired QP fields are assumed to belong to a prescribed subspace,

$$\mathcal{T}(f) = \{v_t^{\mathcal{T}}(x,y;f)\}_{t=1}^{T(f)}, \tag{4}$$

where the $v_t^{\mathcal{T}}(x,y;f)$'s form an orthonormal basis and $T(f)$ is the space dimension of $\mathcal{T}(f)$.

C. Formulation of the Dimensioning Problem

Ideally, one would require $\mathcal{P}(f)$ to contain $\mathcal{T}(f)$ so that all fields of interest could be radiated by the panel. From this point of view, the design task reduces to selecting the panel dimension so that $\mathcal{P}(f)$ is the smallest effective subspace that can approximate $\mathcal{T}(f)$ with an error typically tolerated in this kind of applications, see [10].

In the PWG scenario considered here, the target field on the QP at each frequency is a solitary plane wave. Hence, $T(f) = 1$ and $\mathcal{T}(f)$ is one-dimensional, spanned by a plane-wave function. The key objective is then to ensure that $\mathcal{P}(f)$ is sufficient to approximate this target subspace across the operational frequency band.

III. Dimensioning at a Fixed Frequency

Following [2], we first address the single-frequency case, postponing the multi-frequency extension to the next Section. To simplify notation, the explicit frequency dependence of the quantities involved will be temporarily omitted.

Let $E(x,y)$ be a generic field in the target subspace $\mathcal{T}$:

$$E(x,y) = \sum_{t=1}^{T} c_t\, v_t^{\mathcal{T}}(x,y), \tag{5}$$

with unit norm, i.e., $\|E\|_{\mathcal{L}^2(\mathcal{D})} = 1$. This implies $\|\underline{c}\| = 1$, where $\underline{c} = [c_1, \ldots, c_T]^T$ [2].

The best representation of E on the panel is its orthogonal projection onto the subspace $\mathcal{P}$:

$$E^{(Pr)}(x,y) = \sum_{p=1}^{P} \langle E, v_p^{\mathcal{A}_f}\rangle_{\mathcal{L}^2(\mathcal{D})}\, v_p^{\mathcal{A}_f}(x,y), \tag{6}$$

where $\langle\cdot,\cdot\rangle_{\mathcal{L}^2(\mathcal{D})}$ denotes the inner product on the space of square integrable functions on $\mathcal{D}$ denoted by $\mathcal{L}^2(\mathcal{D})$. The corresponding squared error is

$$\mathcal{E}(\underline{c}; a') = \|E - E^{(Pr)}\|^2_{\mathcal{L}^2(\mathcal{D})}. \tag{7}$$

Since $\|E\| = 1$, the error in (7) can be interpreted as relative. According to [2], the error admits the quadratic form

$$\mathcal{E}(\underline{c}; a') = 1 - \underline{c}^H\, \underline{\underline{A}}\, \underline{c}, \tag{8}$$

where $\underline{\underline{A}}$ is a $T \times T$ Hermitian matrix with entries

$$A_{mn} = \sum_{p=1}^{P} \langle v_m^{\mathcal{T}}, v_p^{\mathcal{P}}\rangle_{\mathcal{L}^2(\mathcal{D})}\, \langle v_n^{\mathcal{T}}, v_p^{\mathcal{P}}\rangle^*_{\mathcal{L}^2(\mathcal{D})}, \tag{9}$$

and $(\cdot)^*$ denotes complex conjugation.

For the sake of simplicity, in this work we consider a square Quiet Plane (QP), $a = b$.

When the target subspace is one-dimensional, i.e., $T = 1$, the desired QP field reduces to $E_{\text{target}}(x,y)$. Then, $\underline{\underline{A}}$ reduces to the scalar A_{11}, equal to the squared norm of the projection $\mathcal{P}^{(Pr)}(E_{\text{target}})$ of E_{target} onto $\mathcal{P}$, and the error simplifies to

$$\mathcal{E}'(a') = 1 - \|\mathcal{P}^{(Pr)}(E_{\text{target}})\|^2_{\mathcal{L}^2(\mathcal{D})}. \tag{10}$$

The coefficients of this projection, $\langle v_1^{\mathcal{T}}, v_p^{\mathcal{A}_f}\rangle$, $p = 1, \ldots, P$, represent the required QP field components. Recovering the corresponding source distribution J, e.g., through a truncated SVD, then specifies the panel excitation [11].

As a' increases, the dimension of $\mathcal{P}$ grows, improving its ability to approximate $\mathcal{T}$ and thus monotonically reducing the error $\mathcal{E}'(a')$. The optimal size is therefore determined as the smallest a' such that

$$\mathcal{E}'(a') \leq \overline{\mathcal{E}}', \tag{11}$$

where $\overline{\mathcal{E}}'$ is a prescribed tolerance.

IV. Dimensioning over a Frequency Band

The extension to the multi-frequency case is obtained by repeating the above procedure at each frequency $f \in \mathcal{B}$. Denoting by $a'(f)$ the minimal panel dimension satisfying (11) at frequency f, the final panel size is chosen as

$$a' = \max_{f \in \mathcal{B}} a'(f), \tag{12}$$

thus ensuring compliance with the error constraint across the whole operational band.

V. Numerical Results

In this Section, we provide a first numerical assessment of the presented dimensioning strategy.
In particular, we focus on the synthesis of a plane wave propagating along the positive z-axis, within the band $\mathcal{B} = [900\,\text{MHz}, 9\,\text{GHz}]$. A spherical QZ of radius $a_R = 16$cm has been selected, centered at a distance $d = 63.3$cm from the radiating panel. Such dimensions are of interest in practical applications, see, for example, [5], [6]. The constraint domain $\mathcal{D}$ has been modeled as a square QP with size $2a \times 2b = 64 \times 64\,\text{cm}^2$. When expressed in terms of minimum and maximum wavelengths $\lambda_{\min}$ and $\lambda_{\max}$, respectively, the above parameters correspond to $a_R = 0.48\lambda_{\max} = 4.8\lambda_{\min}$, $d = 1.9\,\lambda_{\max} = 19\,\lambda_{\min}$, and $2a = 2b = 1.92\lambda_{\max} = 19.2\lambda_{\min}$. The dimensioning procedure yields an optimal panel radius of $R = 56.7$cm, corresponding to $2a' = 1.7\lambda_{\max} = 17\lambda_{\min}$. This ensures that condition (11) is satisfied across the entire band.
Figs. 2 and 3 show the amplitude distribution of the panel current needed to the plane wave radiation at the lowest and highest frequencies, respectively, while Figs. 4 and 5 illustrate the corresponding phase distributions.
The accuracy of the synthesized plane wave in the QZ is now quantified in terms of amplitude and phase errors. Figs. 6, 7, 8 and 9 report the error maps at $f_{\min}$ of cuts along the (x, y) plane (Figs. 6 and 8) and along the (x, z) plane (Figs. 7 and 9) for the amplitude and phase. As it can be seen, the maximum amplitude error is confined to less than $\pm 0.5dB$ while the maximum phase error is confined to less than $\pm 5°$ for the phase, thus compliant with typical requirements of the present application [10]. (y, z) cuts are not shown being analogous to (x, z) cuts for symmetry. Figs. 10, 11, 12 and 13 show analogous results at $f_{\max}$. It should be noticed that finding a relation between the maximum amplitude and phase errors across the QZ and the $\mathcal{L}^2(\mathcal{D})$ norm employed to set the desired performance in (11) is non trivial. Accordingly, a fixed $\overline{\mathcal{E}}'$ can lead to maximum errors well below the maximum tolerated ones [10].
Finally, the overall performance of the dimensioned panel is summarized in Figs. 14 and 15, which display the minimum and maximum errors observed within the whole QZ, across the frequency band. These curves demonstrate that both amplitude and phase errors remain globally below the thresholds typically required in PWG applications [10].

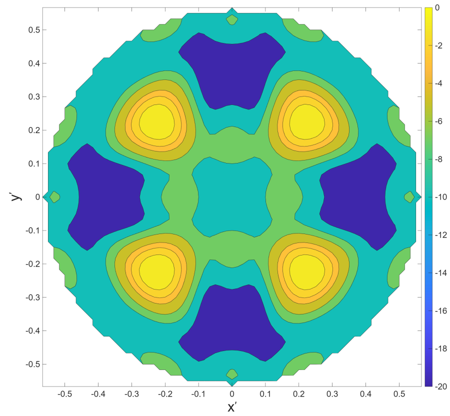

Fig. 2. Amplitude distribution of the panel current J at $f_{\min}$.

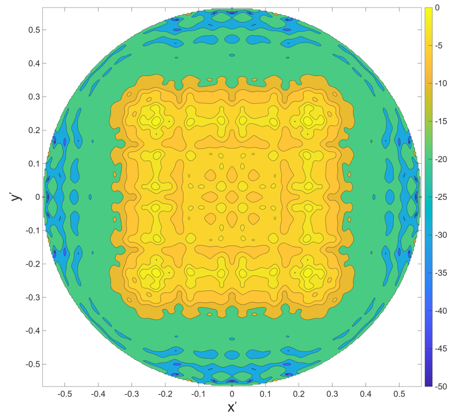

Fig. 3. Amplitude distribution of the panel current J at $f_{\max}$.

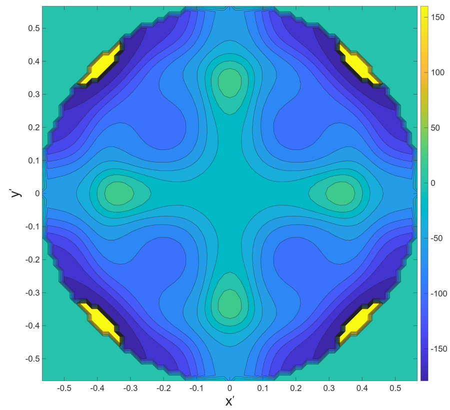

Fig. 4. Phase distribution of the panel current J at $f_{\min}$.

VI. Conclusions and Future Developments

We have dealt with the problem of determining the dimension of a flat and circular radiating panel capable to generate multi-frequency plane waves of interest over a Quiet Zone. The goal has been pursued by enforcing design specifications over a constraint region, the Quiet Plane.
We have considered the particular case of a flat radiating panel of circular shape and a spherical QZ, with a flat and

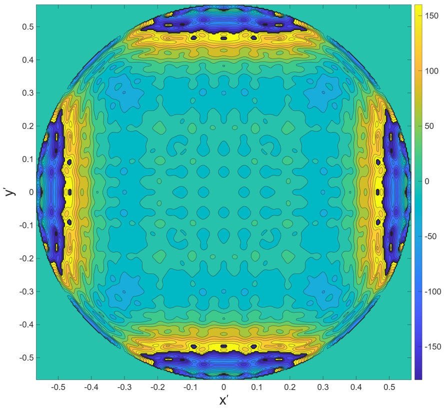

Fig. 5. Phase distribution of the panel current J at $f_{\max}$.

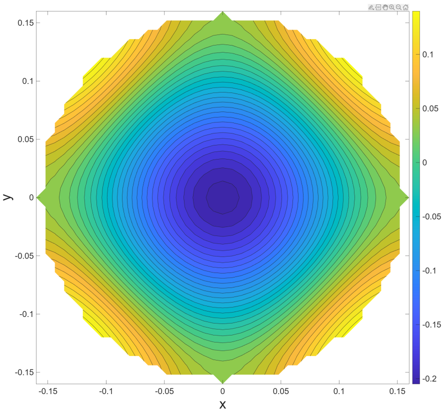

Fig. 6. Cut, along the (x, y) plane, of the amplitude error of the QZ field at $f_{\min}$.

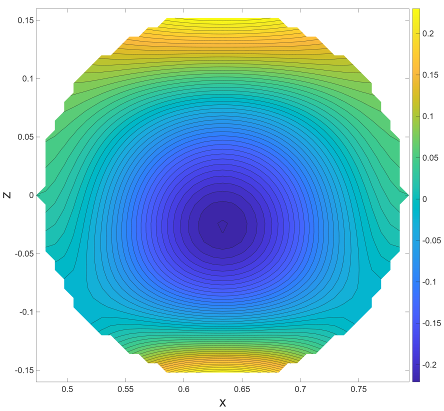

Fig. 7. Cut, along the (x, z) plane, of the amplitude error of the QZ field at $f_{\min}$.

rectangular Quiet Plane. The proposed approach, drawn from [2], has been applied to a case of interest for multi-frequency plane wave generators.

The numerical results have shown the satisfactory performance of the technique.

We finally remark that the continuous radiating panel considered in the paper can be discretized by following the ideas in

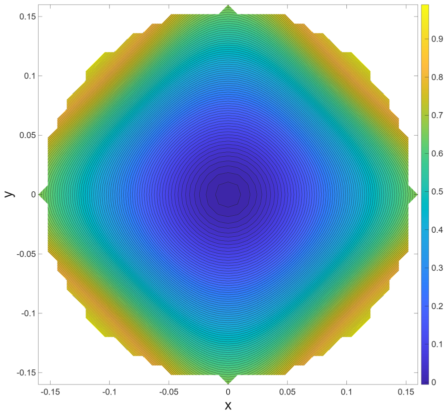

Fig. 8. Cut, along the (x, y) plane, of the phase error of the QZ field at $f_{\min}$.

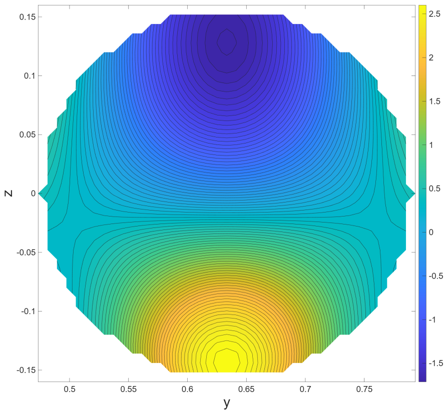

Fig. 9. Cut, along the (x, z) plane, of the phase error of the QZ field at $f_{\min}$.

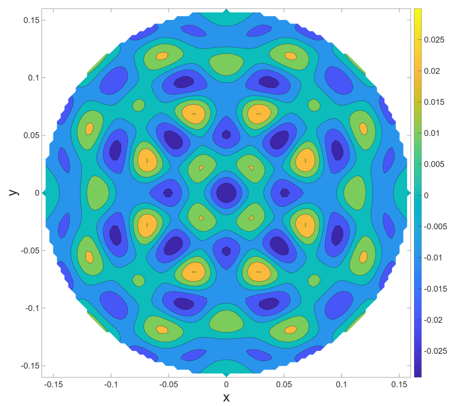

Fig. 10. Cut, along the (x, y) plane, of the amplitude error of the QZ field at $f_{\max}$.

provided in [12], [13].

REFERENCES

[1] A. Capozzoli, C. Curcio, A. Liseno, "Time-harmonic echo generation," *IEEE Trans. Antennas Prop.*, vol. 59, n. 9, pp. 3234–3245, Sep. 2011.

[2] A. Capozzoli, C. Curcio, A. Liseno, "Dimensioning flat equivalent radiators," *IEEE Trans. Antennas Prop.*, vol. 71, n. 7, pp. 5981-5993, Jul. 2023.

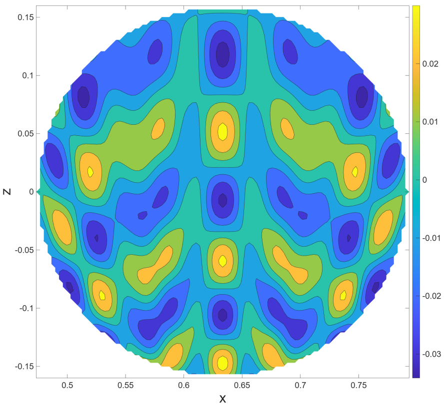

Fig. 11. Cut, along the (x, z) plane, of the amplitude error of the QZ field at $f_{\max}$.

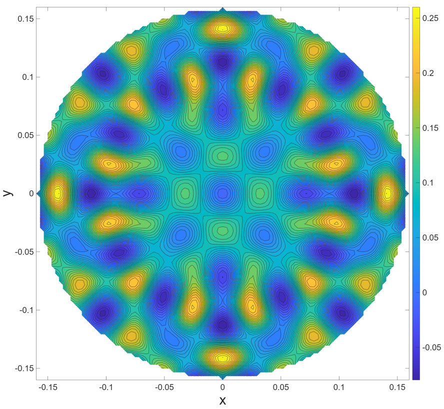

Fig. 12. Cut, along the (x, y) plane, of the phase error of the QZ field at $f_{\max}$.

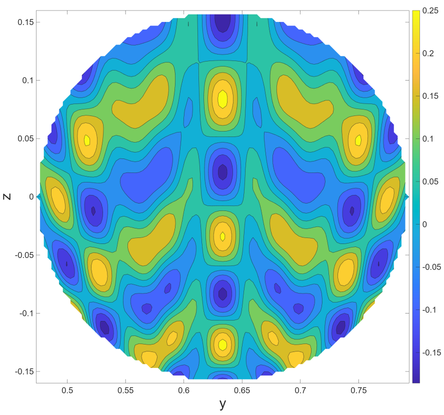

Fig. 13. Cut, along the (x, z) plane, of the phase error of the QZ field at $f_{\max}$.

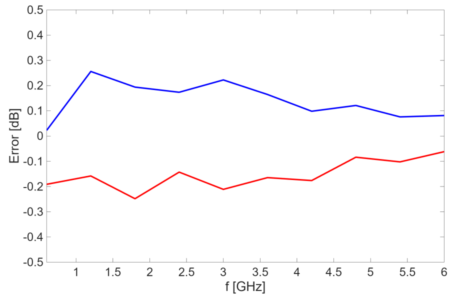

Fig. 14. Minimum and maximum amplitude errors across the QZ, for all $f \in \mathcal{B}$.

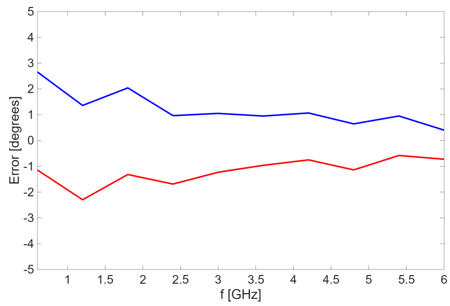

Fig. 15. Minimum and maximum phase errors across the QZ, for all $f \in \mathcal{B}$.

[3] D.J. Belgiovane, C.-C. Chen, S.Y.-P. Chien, R. Sherony, "Surrogate bicycle design for millimeter-wave automotive radar pre-collision testing," *IEEE Trans. Intell. Transp. Syst.*, vol. 18, n. 9, pp. 2413–2422, Sep. 2017.

[4] J.-R. Regue, M. Ribo, J.-M. Garrell, A. Martin, "A genetic algorithm based method for source identification and far-field radiated emissions prediction from near-field measurements for PCB characterization," *IEEE Trans. Electromagn. Compat.*, vol. 43, n. 4, pp. 520–530, Nov. 2001.

[5] V. Schirosi, F. Saccardi, A. Giacomini, F. Scattone, L. Scialacqua, A. Diamanti, E. Tartaglino, L.J. Foged, N. Gross, E. Kaverine, P.O. Iversen, E. Szpindor, "Accurate antenna characterisation at VHF/UHF frequencies with plane wave generator systems," *Proc. of the 2023 Antenna Measurement Teach. Ass. Symp. (AMTA)*, Renton, WA, USA, Oct. 8-13, 2023, pp. 1-6.

[6] F. Scattone, D. Sekuljica, A. Giacomini, F. Saccardi, A. Scannavini, N. Gross, E. Kaverine, P. O. Iversen, L. J. Foged, "Design of dual polarised wide band plane wave generator for direct far-field testing," *Proc. of the 13th Europ. Conf. on Antennas Prop. (EuCAP)*, Krakow, Poland, Mar. 31-Apr. 5, 2019, pp. 1-4.

[7] Antennas and Propagation Standards Committee, "IEEE recommended practice for antenna measurements," *IEEE Std 149-2021*, Approved Sept. 23, 2021.

[8] A. Capozzoli, C. Curcio, L. Foged, A. Liseno, F. Saccardi, "Dimensioning of flat radiating panels for plane-wave generation," *Proc. of the Int. Conf. on Electromagn. in Adv. Appl. (ICEAA)*, Palermo, Italy, Sept. 8-12, 2025, pp. 1-5.

[9] A. Capozzoli, C. Curcio, A. Liseno, "Controlling the field levels outside the Quiet Plane in the design of 1D complex waveform generators," *Proc. of the IEEE Int. Symp. on Antennas Prop.*, Ottawa, Canada, Jul. 13-18, 2025, pp. 1-3.

[10] A.W. Rudge, K. Milne, A.D. Olver, P. Knight, *T*he Handbook of Antenna Design, London: Peter Peregrinus, 1982.

[11] A. Capozzoli, C. Curcio, A. Liseno, "Different metrics for singular value optimization in near-field antenna characterization,"*Sensors*, vol. 21, n. 6, art. no. 2122, pp. 1 - 15, 2021.

[12] A. Capozzoli, C. Curcio, F. D'Agostino, A. Liseno, L. Pascarella, "Legendre quadrature for the discretization of 1D radiating panels,"*Int. J. Microw. Wireless Tech.*, vol. 16, n. 1, pp. 49-54, Feb. 2024.

[13] A. Capozzoli, C. Curcio, F. D'Agostino, A. Liseno, L. Pascarella, "Generalized quadrature rules for the discretization of 1D radiating ianels,"*Microw. Opt. Tech. Lett.*, vol. 67, n. 3, pp. 1-6, Mar. 2025.